

An Analysis of Concentration Profiles for Fluxes, Diffusion Depths, and Zero-Flux Planes in Multicomponent Diffusion

M. A. DAYANANDA

Concentration profiles developed during isothermal, multicomponent diffusion for a single-phase, solid-solid diffusion couple are expressed on the basis of a relative concentration variable for each component and analyzed for the determination of interdiffusion fluxes. The individual concentration profiles intersect at a common cross-over composition where the relative concentrations of all components are identical. New relations are developed for describing internal consistency among the concentration profiles of the various components. A link is made between the cross-over composition and the depths of the diffusion zone on either side of the Matano plane for a diffusion couple. The cross-over composition is interpreted as the average relative concentration of each component over the diffusion zone. The identification of a zero-flux plane from concentration profiles is also described. The analysis offers several advantages in presenting as well as checking the self-consistency of results as illustrated with a single phase Cu-Ni-Zn diffusion couple annealed at 775 °C.

I. INTRODUCTION

ONE of the main objectives of isothermal ternary diffusion studies is the experimental determination of concentration dependent diffusion data such as interdiffusion coefficients and intrinsic diffusion coefficients on the basis of Onsager's formalism¹ of Fick's law extended to multicomponent diffusion. In literature exist several diffusion studies that report data on ternary interdiffusion coefficients²⁻¹⁸ and intrinsic diffusion coefficients^{3,5,8,11,16,19} for various ternary systems. Most of these studies have employed independent diffusion couples of the solid-solid or vapor-solid type with intersecting diffusion paths for the determination of ternary diffusion coefficients at the common composition points of couple pairs. For an n -component system, $(n - 1)$ independent diffusion couples are needed, in general, for the determination of $(n - 1)^2$ interdiffusion coefficients at one composition.

Appreciable insight has also been developed into the development of concentration profiles and diffusion paths for single phase ternary diffusion couples. One-dimensional solutions to ternary diffusion equations are available for both solid-solid^{2,20-22} and vapor-solid^{23,24} couples; among them are those that assume constant diagonal and cross coefficients or constant diagonal but variable cross coefficients. Alternative approaches based on simple concepts of penetration tendencies²⁵ for the individual components are also available and provide a partial insight into the s -shape of diffusion paths for solid-solid couples. Analytical representation of diffusion paths based on two characteristic path parameters has also been recently proposed.²⁶

In an earlier paper²⁷ a unidimensional analysis was presented for the direct calculation of interdiffusion fluxes from concentration profiles of semi-infinite couples without the need for a prior knowledge of interdiffusion coefficients. Such flux calculations for diffusion couples in the Cu-Ni-Zn system helped identify the development of zero-flux planes and flux reversals for the individual components within the diffusion zone. These observations implied that

the interdiffusion flux of a component could be in opposite directions in adjacent regions of a multicomponent assembly and could go to zero at a zero-flux plane separating the two regions.

In this paper, the analysis for the calculation of interdiffusion fluxes from concentration profiles of single phase, solid-solid diffusion couples is further developed on the basis of a laboratory-fixed frame by employing a relative concentration variable for each component. Such analysis circumvents the need for the location of the Matano plane and provides additional relations for checking the internal consistency among the concentration profiles of the various components in a multicomponent diffusion assembly. The flux calculations are complementary to and precede the determination of interdiffusion coefficients. On the basis of the relative concentration variable the concentration profiles of all components intersect or cross at a common cross-over composition. A link is also made between the cross-over composition and the depths of the diffusion zones on either side of the Matano plane for the couple. The concentration profiles of a Cu-Ni-Zn ternary diffusion couple developing a zero-flux plane for Ni are examined in the context of the present analysis.

II. INTERDIFFUSION FLUXES FROM CONCENTRATION PROFILES

On the basis of Onsager's formalism¹ of Fick's law, the interdiffusion flux \bar{J}_i of component i referred to a laboratory-fixed frame for unidimensional diffusion in an n -component system can be expressed in terms of $(n - 1)$ independent concentration gradients, $\partial C_j/\partial x$, by:

$$\bar{J}_i = - \sum_{j=1}^{n-1} \bar{D}_{ij}^n \frac{\partial C_j}{\partial x} \quad (i = 1, 2, \dots, n - 1) \quad [1]$$

where $(n - 1)^2$ interdiffusion coefficients \bar{D}_{ij}^n are defined. For a ternary system there exist four concentration dependent interdiffusion coefficients. If data on these coefficients are available, \bar{J}_i 's can be determined from Eq. [1].

An alternative approach bypassing the need for interdiffusion coefficients has been presented²⁷ for the determination of interdiffusion flux \bar{J}_i of component i directly

M. A. DAYANANDA is Professor of Materials Engineering, Purdue University, West Lafayette, IN 47907.

Manuscript submitted November 2, 1982.

from the concentration profiles of a solid-solid diffusion couple in an n -component system. If C_i^+ and C_i^- are the terminal concentrations of component i of the two terminal alloys employed in the couple assembly, \bar{J}_i at any section x^* based on the Matano coordinate is obtained from the relation:

$$\bar{J}_i(x^*) = \frac{1}{2t} \int_{C_i^+}^{C_i(x^*)} (x - x_0) dC_i \quad (i = 1, 2, \dots, n) \quad [2]$$

or from the relation

$$\bar{J}_i(x^*) = \frac{1}{2t} \int_{C_i^-}^{C_i(x^*)} (x - x_0) dC_i \quad (i = 1, 2, \dots, n) \quad [3]$$

where t is the time of diffusion and x_0 is the location of the Matano plane for the couple. In the derivation of Eqs. [2] and [3], C_i 's are functions of the Boltzmann parameter x/\sqrt{t} , and the variation of the molar volume within the diffusion zone is considered negligible.

The concentration profiles of the individual components for a single phase multicomponent diffusion couple with n components may also be analyzed in terms of the relative concentration variable Y_i defined by

$$Y_i = \frac{C_i - C_i^+}{C_i^- - C_i^+} \quad (i = 1, 2, \dots, n) \quad [4]$$

where C_i is the concentration in g · moles/cc of component i at any section of the diffusion zone. Figure 1 shows a schematic concentration profile for component i as a plot of Y_i as a function of distance x over the diffusion zone between L^- to L^+ . The Matano plane for the couple is located at x_0 on the basis of the mass balance expressed in terms of the areas in the figure by

$$E = A + B + C \quad [5]$$

Hence, for a given section x^* it follows from the figure

$$E + D = A + B + C + D$$

or

$$(E + D) - A = (B + C + D)$$

or

$$\int_{L^-}^{x^*} (1 - Y_i) dx - \int_{x^*}^{L^+} Y_i dx = (x^* - x_0) \quad (i = 1, 2, \dots, n) \quad [6]$$

since

$$E + D = \int_{L^-}^{x^*} (1 - Y_i) dx; \quad A = \int_{x^*}^{L^+} Y_i dx$$

and

$$(B + C + D) = (x^* - x_0)$$

In terms of Y_i Eq. [2] can be written as:

$$\begin{aligned} \bar{J}_i(x^*) &= \frac{\Delta C_i}{2t} \int_0^{Y_i^*} (x - x_0) dY_i \\ &= \frac{\Delta C_i}{2t} \left[(x^* - x_0) Y_i^* + \int_{x^*}^{L^+} Y_i dx \right] \end{aligned} \quad (i = 1, 2, \dots, n) \quad [7]$$

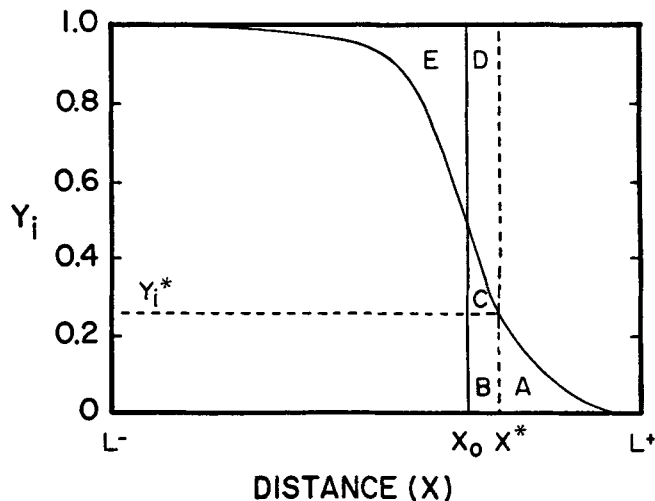


Fig. 1— Schematic concentration profile of component i shown as a plot of relative concentration Y_i vs distance x . x_0 refers to the location of the Matano plane.

where $\Delta C_i = (C_i^- - C_i^+)$. Similarly, Eq. [3] can be written in terms of $(1 - Y_i)$ by:

$$\begin{aligned} \bar{J}_i(x^*) &= \frac{\Delta C_i}{2t} \left[\int_0^{(1-Y_i^*)} (x_0 - x) d(1 - Y_i) \right] \\ &= \frac{\Delta C_i}{2t} \left[(x_0 - x^*) (1 - Y_i^*) + \int_{L^-}^{x^*} (1 - Y_i) dx \right] \end{aligned} \quad (i = 1, 2, \dots, n) \quad [8]$$

On substitution of Eq. [6] in Eq. [7], one can write the expression for $\bar{J}_i(x^*)$ in another equivalent form given by:

$$\begin{aligned} \bar{J}_i(x^*) &= \frac{\Delta C_i}{2t} \left[Y_i^* \int_{L^-}^{x^*} (1 - Y_i) dx \right. \\ &\quad \left. + (1 - Y_i^*) \int_{x^*}^{L^+} Y_i dx \right] \end{aligned} \quad (i = 1, 2, \dots, n) \quad [9]$$

The use of Eqs. [7] and [8] for the calculation of interdiffusion fluxes requires the location x_0 of the Matano plane. On the other hand, Eq. [9] allows the calculation of fluxes from the concentration profiles without the need for the location of the Matano plane and is particularly useful in the analysis of profiles with maxima and/or minima in concentrations.

For the case where the variation of molar volume V_m with composition cannot be ignored, Eq. [9] can be modified¹⁸ to:

$$\begin{aligned} J_i^M(x^*) &= \frac{\Delta C_i}{2t} \left[Y_i^* \int_{L^-}^{x^*} \frac{(1 - Y_i)}{V_m} dx \right. \\ &\quad \left. + (1 - Y_i^*) \int_{x^*}^{L^+} \frac{Y_i}{V_m} dx \right] \end{aligned} \quad (i = 1, 2, \dots, n) \quad [10]$$

where the flux J_i^M is based on a mole-fixed reference frame. The assumption of constant molar volume will, however, be employed in the analysis to follow.

For the determination of concentration dependent interdiffusion coefficients, Eq. [9] for \bar{J}_i can be combined with Eq. [1] to yield:

$$\left[Y_i^* \int_{L^-}^{x^*} (1 - Y_i) dx + (1 - Y_i^*) \int_{x^*}^{L^+} Y_i dx \right] = -2t \sum_{j=1}^{n-1} \bar{D}_{ij}^n \frac{\partial Y_j}{\partial x} \quad (i = 1, 2, \dots, n) \quad [11]$$

Equation [11] requires $(n - 1)$ couples with diffusion paths intersecting at a common composition for the determination of $(n - 1)^2$ interdiffusion coefficients. The use of Eq. [11] without needing the location of x_0 has been discussed^{28,29} in the context of the determination of diffusion coefficients in binary and ternary alloys. If Eq. [2] for \bar{J}_i is combined with Eq. [1] one gets:

$$\int_{C_i^-}^{C_i(x^*)} (x - x_0) dC_i = -2t \left[\sum_{j=1}^{n-1} \bar{D}_{ij}^n \frac{\partial C_i}{\partial x} \right]_{C_i(x^*)} \quad [12]$$

Equation [12] has been the basis for the determination of concentration dependent interdiffusion coefficients in ternary systems²⁻¹⁸ with pairs of diffusion couples having intersecting diffusion paths. Equations [11] and [12] imply that the calculation of interdiffusion coefficients needs the determination of interdiffusion fluxes.

III. CONCENTRATION PROFILES AND FLUX PROFILES FOR A Cu-Ni-Zn DIFFUSION COUPLE

The use of the Y_i parameter for the concentration profiles and the calculation of fluxes from the profiles are illustrated with a single phase (fcc) ternary Cu-Ni-Zn diffusion couple. The couple was assembled with disks of Alloy I (30.1Cu-44.7Ni-25.2Zn at.pct) and Alloy II (80.6Cu-19.4Ni) and diffusion annealed at 775 °C for two days. The experimental concentration profiles for the couple are presented as plots of atom fraction vs x as well as plots of Y_i vs x in Figure 2. C_i^- and C_i^+ have been identified with the concentrations of the components in Alloy I and Alloy II, respectively. The interdiffusion fluxes \bar{J}_i based on the Matano coordinate calculated from the profiles on the basis of Eq. [9] are presented as flux profiles over the diffusion zone in Figure 3. The fluxes can be expressed in units of $g \cdot \text{moles}/\text{cm}^2 \cdot \text{sec}$ by dividing the values in Figure 3 by the molar volume of 7.1 $\text{cc}/\text{g} \cdot \text{mole}$ ³⁰ taken as constant over the composition range of the couple. Figures 2 and 3 exhibit several important features that will be discussed in the following sections.

IV. COMMON RELATIVE CONCENTRATION Y_c

One of the important advantages in using the Y_i variable as defined by Eq. [4] is that the concentration profiles of all components can be displayed together over the diffusion zone L^- to L^+ so that Y_i is 1 at L^- and is zero at L^+ for all components regardless of their flow directions within the diffusion zone, as shown in Figure 2(b). Such a presentation is helpful in the location of the Matano plane x_0 from the individual profiles and in cross-checking to see if their locations match as expected on the basis of negligible variation in molar volume.

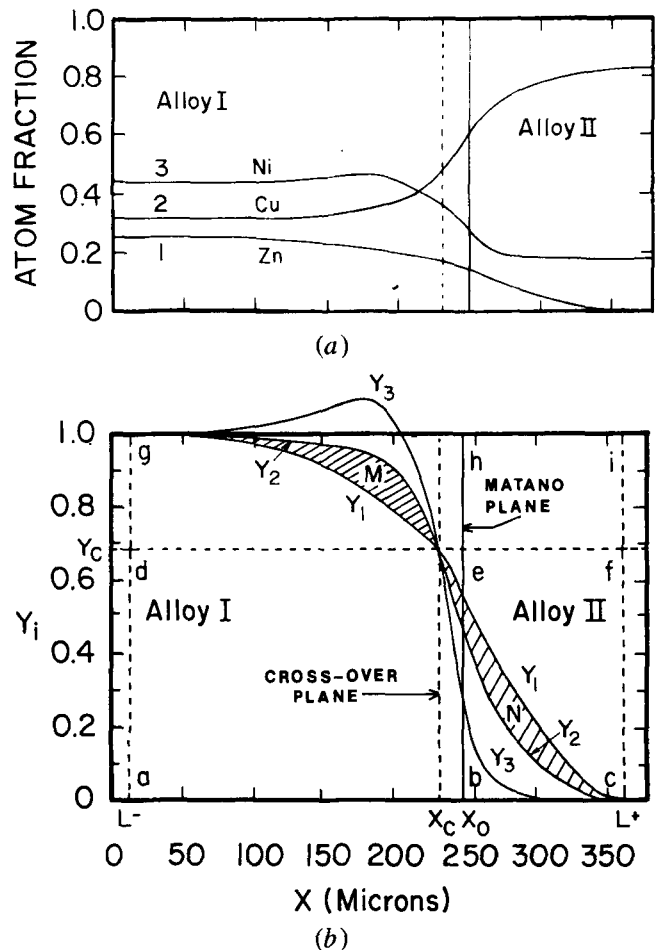


Fig. 2— Concentration profiles of a ternary diffusion couple assembled with Alloy I (30.1Cu-44.7Ni-25.2Zn, at. pct) and Alloy II (80.6Cu-19.4Ni) and diffusion annealed at 775 °C for 2 days; concentrations are expressed (a) in atom fraction and (b) in relative concentration Y_i . x_0 and x_c refer to the locations of the Matano plane and the cross-over plane, respectively. Y_c is the common relative concentration for all components at the cross-over plane.

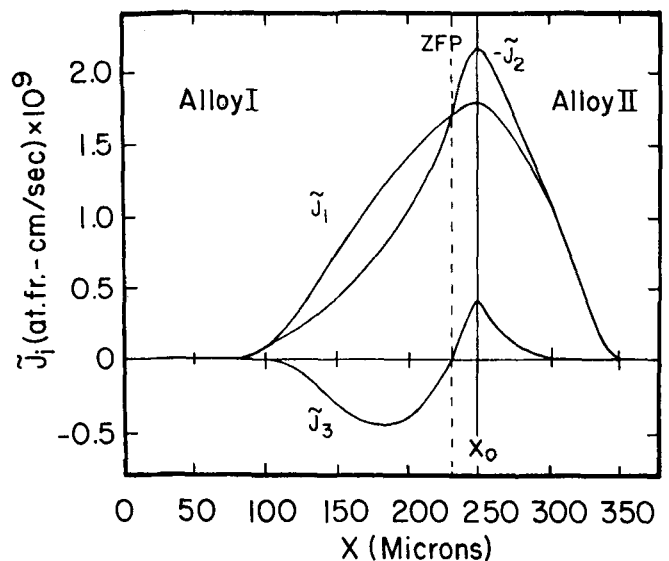


Fig. 3— Calculated interdiffusion fluxes within the diffusion zone for the couple Alloy I vs Alloy II. Components 1, 2, and 3 refer to Zn, Cu, and Ni, respectively. The direction from Alloy I to Alloy II is taken as the positive direction for fluxes. Note the plot of $-\bar{J}_2$ for convenience.

Another important feature of the Y_i vs x plots is the mutual crossing of the various profiles at a common relative concentration Y_c at the cross-over plane x_c as identified in Figure 2(b). At x_c , $Y_i = Y_c$ for all i . This composition can be appreciated better with the aid of the diffusion path for the couple shown as a plot of Y_{Zn} as a function of Y_{Cu} in Figure 4. It can be seen that Y_c corresponds to the cross-over composition of the diffusion path intersecting the straight line, $Y_{Zn} = Y_{Cu}$ drawn between the terminal compositions represented by the points $Y_i = 0$ for Alloy II and $Y_i = 1$ for Alloy I of the diffusion couple. Y_c and the slope of the path at Y_c are considered two characteristic parameters for the couple. These parameters are found to be dependent on $\Delta C_1/\Delta C_2$, the ratio of the concentration differences for any two components in the terminal alloys of the couple. Based on Y_c and the path slope at Y_c , an approach for the analytical representation and prediction of the diffusion path has been discussed in a recent paper.²⁶ For the path in Figure 4, Y_c equals 0.68 and the path slope dY_{Zn}/dY_{Cu} at Y_c is 0.417.

V. CONSISTENCY RELATIONS FOR PROFILES

Relations for checking the consistency or acceptability of the experimental profiles as shown in Figure 2(b) can be developed on the basis of Eq. [6], which is valid at any section x for each of the components. On writing Eq. [6] at section x for two components, one gets:

$$\int_{L^-}^x (1 - Y_1) dx - \int_x^{L^+} Y_1 dx = \int_{L^-}^x (1 - Y_2) dx - \int_x^{L^+} Y_2 dx \quad [13]$$

where components 1 and 2 may be identified with Zn and Cu, respectively. Alternatively, Eq. [13] becomes:

$$\int_{L^-}^x (Y_2 - Y_1) dx = \int_x^{L^+} (Y_1 - Y_2) dx \quad [14]$$

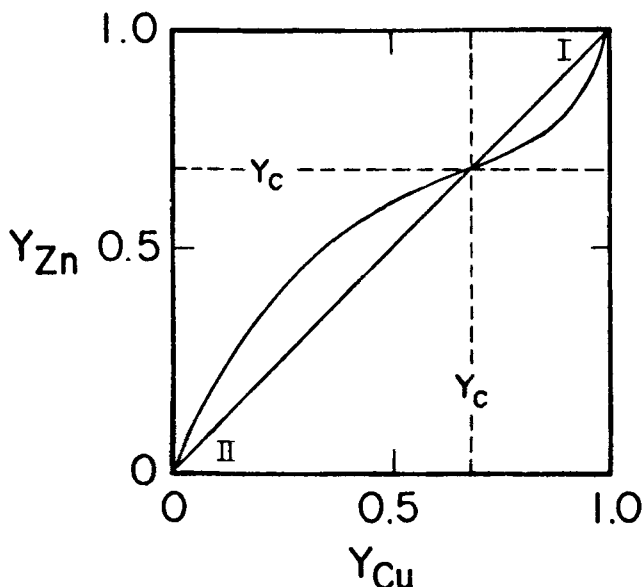


Fig. 4— Diffusion path for the couple Alloy I vs Alloy II shown as a composition plot of relative concentration of one component vs that of another. Y_c corresponds to the cross-over composition and equals 0.68.

or

$$\int_{L^-}^{L^+} (Y_1 - Y_2) dx = 0 \quad [15]$$

At x_c corresponding to the concentration Y_c in Figure 2, Eq. [14] yields:

$$\int_{L^-}^{x_c} (Y_2 - Y_1) dx = \int_{x_c}^{L^+} (Y_1 - Y_2) dx \quad [16]$$

Equation [16] implies that the areas M and N in Figure 2(b) should be equal. Relations similar to Eq. [15] or Eq. [16] can be written for any two of the components i and j and hence, in general

$$\int_{L^-}^{L^+} (Y_i - Y_j) dx = 0 \quad (i, j = 1, 2, 3; i \neq j) \quad [17]$$

Equation [17] requires that the area between the profiles of relative concentrations of any two components for a single phase multicomponent diffusion couple must be identical on either side of Y_c . This requirement is quite useful in ascertaining if the experimental profiles are satisfactory over the entire diffusion zone in a multicomponent system. Relations given by Eq. [17] may be designated as consistency relations for the concentration profiles.

The magnitude of the area M or N in Figure 2(b) is given by the integral

$$\int_{x_c}^{L^+} (Y_1 - Y_2) dx$$

from Eq. [16]. This integral can be expressed in terms of the fluxes \bar{J}_1 and \bar{J}_2 at x_c . On writing Eq. [7] for \bar{J}_1 and \bar{J}_2 at x_c , where $Y_1 = Y_2 = Y_c$ and subtracting one equation from the other, one gets

$$\left[\frac{\bar{J}_1}{\Delta C_1} - \frac{\bar{J}_2}{\Delta C_2} \right]_{x_c} = \frac{1}{2t} \int_{x_c}^{L^+} (Y_1 - Y_2) dx \quad [18]$$

Equation [18] implies that the area between the concentration profiles of any two components on either side of x_c in the Y_i vs x plots relates directly to the difference in the interdiffusion fluxes of the two components at x_c weighted by appropriate ΔC_i factors.

A simple criterion for the location of x_c can be found from a consideration of the integral $I(x)$ given by:

$$I(x) = \int_x^{L^+} (Y_i - Y_j) dx \quad (i \neq j)$$

The value of this integral is a maximum or a minimum for $x = x_c$, since $Y_i = Y_j = Y_c$ at x_c , $I(L^+)$ and $I(L^-)$ are zero and

$$\frac{d}{dx} \left[\int_x^{L^+} (Y_i - Y_j) dx \right]_{x_c} = Y_j - Y_i = 0$$

As is evident from the area M or N in Figure 2(b), the magnitude of the integral $I(x_c)$ corresponds to a maximum for any choice of i and j components.

VI. LOCATION OF CROSS-OVER PLANE

An expression for the location of the cross-over plane relative to the Matano plane given by $(x_c - x_0)$ can be derived in terms of areas represented by the integrals

$$\int_{x_c}^{L^+} Y_i dx \quad \text{and} \quad \int_{L^-}^{x_c} (1 - Y_i) dx$$

Equation [9] can be written for any two components 1 and 2 at the section x_c , and the two equations can be solved simultaneously for Y_c and $(1 - Y_c)$ to get:

$$Y_c = \frac{\frac{\bar{J}_2 2t}{\Delta C_2} \int_{x_c}^{L^+} Y_1 dx - \frac{\bar{J}_1 2t}{\Delta C_1} \int_{x_c}^{L^+} Y_2 dx}{\int_{x_c}^{L^+} Y_1 dx \cdot \int_{L^-}^{x_c} (1 - Y_2) dx - \int_{x_c}^{L^+} Y_2 dx \cdot \int_{L^-}^{x_c} (1 - Y_1) dx} \quad [19]$$

and

$$(1 - Y_c) = \frac{\frac{\bar{J}_1 2t}{\Delta C_1} \int_{L^-}^{x_c} (1 - Y_2) dx - \frac{\bar{J}_2 2t}{\Delta C_2} \int_{L^-}^{x_c} (1 - Y_1) dx}{\int_{x_c}^{L^+} Y_1 dx \cdot \int_{L^-}^{x_c} (1 - Y_2) dx - \int_{x_c}^{L^+} Y_2 dx \cdot \int_{L^-}^{x_c} (1 - Y_1) dx} \quad [20]$$

On substituting Eq. [19] in Eq. [20] and making use of Eqs. [6] and [13], one gets:

$$(x_c - x_0) = \frac{\int_{x_c}^{L^+} Y_1 dx \cdot \int_{L^-}^{x_c} (1 - Y_2) dx - \int_{x_c}^{L^+} Y_2 dx \cdot \int_{L^-}^{x_c} (1 - Y_1) dx}{\left[\frac{\bar{J}_1 2t}{\Delta C_1} \right]_{x_c} - \left[\frac{\bar{J}_2 2t}{\Delta C_2} \right]_{x_c}} \quad [21]$$

Substitution of Eq. [18] in Eq. [21] yields:

$$(x_c - x_0) = \frac{\int_{x_c}^{L^+} Y_1 dx \cdot \int_{L^-}^{x_c} (1 - Y_2) dx - \int_{x_c}^{L^+} Y_2 dx \cdot \int_{L^-}^{x_c} (1 - Y_1) dx}{\int_{x_c}^{L^+} (Y_1 - Y_2) dx} \quad [22]$$

Equation [22] clearly indicates that the location x_c of the cross-over plane relative to that of the Matano plane is related to the concentration profiles of any two components on either side of x_c .

VII. RELATION OF Y_c TO DIFFUSION DEPTHS

The cross-over composition Y_c where the relative concentrations of all components are identical can be described in terms of the relative depths of the diffusion zone on either side of the Matano plane. In Figure 2(b) the locations of L^- and L^+ are selected to cover the effective diffusion zone of the couple so that $Y_i = 1$ at L^- and $Y_i = 0$ at L^+ for all i . For a given location of L^- and L^+ it can be seen from the figure that for each component i , the mass balance requires:

$$\begin{aligned} \int_{L^-}^{L^+} Y_i dx &= \text{area } abhg \\ &= x_0 - L^- \quad (i = 1, 2, \dots, n) \quad [23] \end{aligned}$$

Similarly,

$$\begin{aligned} \int_{L^-}^{L^+} (1 - Y_i) dx &= \text{area } bcih \\ &= L^+ - x_0 \quad (i = 1, 2, \dots, n) \quad [24] \end{aligned}$$

The locations of L^- and L^+ can be conveniently chosen so that area $abhg$ equals area $acfd$ and area $bcih$ equals area $dfig$. Then,

$$x_0 - L^- = Y_c(L^+ - L^-) \quad [25]$$

and

$$(L^+ - x_0) = (1 - Y_c)(L^+ - L^-) \quad [26]$$

Hence, it follows that

$$\frac{Y_c}{1 - Y_c} = \frac{x_0 - L^-}{L^+ - x_0} \quad [27]$$

or, alternatively, area $dehg$ equals area $bcfe$. In other words, Y_c and $1 - Y_c$ can be considered to be proportional to the effective depths of the diffusion zone, $(x_0 - L^-)$ and $(L^+ - x_0)$, respectively, on either side of x_0 for the couple for a given time of diffusion. These diffusion depths are considered to be characteristic of the two alloys on either side of x_0 , only when they are assembled together in the form of a solid-solid diffusion couple and the ratio of the depths is invariant with time.

On the basis of Eqs. [23] and [25] Y_c is expressed by

$$Y_c = \frac{1}{(L^+ - L^-)} \int_{L^-}^{L^+} Y_i dx \quad (i = 1, 2, \dots, n) \quad [28]$$

and from Eqs. [24] and [26], $(1 - Y_c)$ is given by

$$(1 - Y_c) = \frac{1}{(L^+ - L^-)} \int_{L^-}^{L^+} (1 - Y_i) dx \quad (i = 1, 2, \dots, n) \quad [29]$$

These equations imply that Y_c can be interpreted as the average relative concentration of any component over the total diffusion zone ($L^+ - L^-$) for the couple and is the same for all components regardless of their diffusion directions within the diffusion zone. Equations [28] and [29] hold for all choices of L^- and L^+ satisfying Eq. [27]. Also, the diffusion zone ($L^+ - L^-$) is defined for the couple and is the same for all components. Hence, Y_c , as a characteristic parameter for the diffusion couple, reflects the average composition of the diffusion zone. In addition, Y_c and $(1 - Y_c)$ can be interpreted as the relative depths of the diffusion zone on either side of the Matano plane. For the couple in Figure 2, a Y_c value of 0.68 reflects the fact that the depth of the diffusion zone on the Alloy I side of the couple is 2.125 times larger than that on the Alloy II side.

VIII. IDENTIFICATION OF ZERO-FLUX PLANES

The flux profiles for the individual components shown in Figure 3 clearly show that the interdiffusion flux of component 1 (Zn) is positive, that is, in the direction from Alloy I to Alloy II, while the flux of component 2 (Cu) is negative in the direction from Alloy II to Alloy I at all sections over the diffusion zone. On the other hand, the component 3 (Ni) exhibits regions of both positive and negative directions for its flux with the transition occurring through a plane where the flux is zero; such a plane is referred to as a zero-flux plane (ZFP) for the component.²⁷

The development of a ZFP for Ni on the Matano coordinate for the couple Alloy I vs Alloy II can be identified from the relative concentration profile of component 3 (Ni) as shown in Figure 5. The profile exhibits a maximum where Y_3 has values greater than 1.0. Since \bar{J}_i is zero at a ZFP for component i , Eq. [7] yields:

$$\bar{J}_i(\text{ZFP}) = \frac{\Delta C_i}{2t} \left[(x_{\text{ZFP}} - x_0)(Y_i)_{\text{ZFP}} + \int_{x_{\text{ZFP}}}^{L^+} Y_i dx \right] = 0$$

Or,

$$(x_0 - x_{\text{ZFP}})(Y_i)_{\text{ZFP}} = \int_{x_{\text{ZFP}}}^{L^+} Y_i dx \quad [30]$$

Equation [30] implies that areas P and Q in Figure 5 are equal in magnitude. Similarly, on the basis of Eq. [8], one can write:

$$(x_{\text{ZFP}} - x_0)(1 - Y_i)_{\text{ZFP}} = \int_{L^-}^{x_{\text{ZFP}}} (1 - Y_i) dx \quad [31]$$

Equation [31] reflects the fact that areas S and R are also equal in magnitude. Equation [31] is not independent of Eq. [30] since the mass balance requirement over the diffusion zone requires that the loss ($R + Q$) must be equal to the gain ($S + P$). The main significance of ZFP lies in the fact that the loss ($R + Q$) on the left-hand side of x_0 will not show up as a gain on the right-hand side of x_0 but is split up into partial gains P and S , one on either side of the Matano plane. In other words, the loss R is equal to the gain S , since the component diffuses from right to left (in the negative direction) to the left of x_{ZFP} , and the loss Q is equal to the gain P , as the component diffuses from left to right (in the positive direction) to the right of x_{ZFP} . Hence, concentration profiles that exhibit a maximum and/or a minimum and

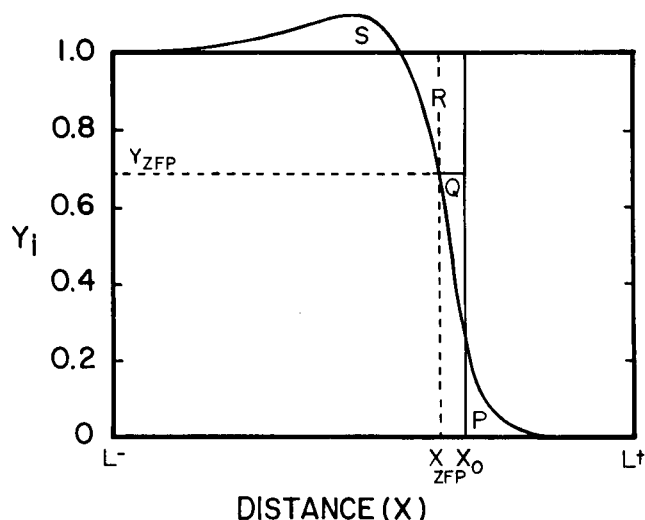


Fig. 5—The concentration profile of Ni (component 3) showing the development of a zero-flux plane (ZFP) for the couple Alloy I vs Alloy II. The ZFP is located by the requirement that area $P = \text{area } Q$ and area $S = \text{area } R$.

indicate equalization of areas as implied by Eqs. [30] and [31] would indicate the presence of a ZFP and flux reversal on the basis of the Matano coordinate.

The concentration of component i at the ZFP is related directly to the concentration profile on either side of x_{ZFP} . On dividing Eq. [30] by Eq. [31] one gets

$$\frac{(Y_i)_{\text{ZFP}}}{(1 - Y_i)_{\text{ZFP}}} = \frac{\int_{x_{\text{ZFP}}}^{L^+} Y_i dx}{\int_{x_{\text{ZFP}}}^{L^+} (1 - Y_i) dx} \quad [32]$$

Equation [32] also follows directly from Eq. [9] since $\bar{J}_i = 0$ at the ZFP.

If component 3 in a ternary diffusion couple develops a ZFP at x_{ZFP} , then one can show from Eq. [7] that the fluxes of the other components 1 and 2 at the ZFP can be expressed by

$$\frac{2i\bar{J}_i}{\Delta C_i} \Big|_{\text{ZFP}} = \int_{x_{\text{ZFP}}}^{L^+} Y_i dx - \left(\frac{Y_i}{Y_3} \right)_{\text{ZFP}} \int_{x_{\text{ZFP}}}^{L^+} Y_3 dx \quad (i = 1, 2) \quad [33]$$

For the couple presented in Figures 2 and 3, the location of ZFP for Ni (component 3) happens to coincide with that of Y_c , i.e., $x_{\text{ZFP}} = x_c$. This is unusual but can happen in multicomponent diffusion as has been observed³¹ in selected diffusion couples in the Cu-Ni-Zn system. In such a case, $(Y_i) = Y_c$ for all components at the ZFP and Eq. [33] yields:

$$\frac{2i\bar{J}_i}{\Delta C_i} \Big|_{\text{ZFP}} = \int_{x_c}^{L^+} (Y_i - Y_3) dx \quad (i = 1, 2) \quad [34]$$

At the Ni ZFP, the interdiffusion fluxes of Zn and Cu are both equal in magnitude but are of opposite signs, as can be seen in Figure 3.

The development of a ZFP also provides direct information on the diffusional interactions among components. For example, if Cu is taken as the dependent concentration variable, Eq. [1] yields for the Ni ZFP in Figure 3:

$$-\bar{D}_{\text{NiNi}}^{\text{Cu}} \frac{\partial C_{\text{Ni}}}{\partial x} - \bar{D}_{\text{NiZn}}^{\text{Cu}} \frac{\partial C_{\text{Zn}}}{\partial x} = 0$$

or

$$\begin{aligned} \frac{\bar{D}_{\text{NiZn}}^{\text{Cu}}}{\bar{D}_{\text{NiNi}}^{\text{Cu}}} &= - \frac{\partial C_{\text{Ni}}}{\partial C_{\text{Zn}}} \Big|_{\text{ZFP for Ni}} \\ &= - \frac{\Delta C_{\text{Ni}}}{\Delta C_{\text{Zn}}} \frac{dY_{\text{Ni}}}{dY_{\text{Zn}}} \Big|_{\text{ZFP for Ni}} \end{aligned} \quad [35]$$

For the Alloy I vs Alloy II couple, $\Delta C_{\text{Ni}}/\Delta C_{\text{Zn}} \approx 1$ and the path slope $dY_{\text{Ni}}/dY_{\text{Zn}}$ at the ZFP for Ni is found to be 4.1. Hence, from Eq. [35] it follows that the cross-coefficient $\bar{D}_{\text{NiZn}}^{\text{Cu}}$ is about four times as large in magnitude but opposite in sign as the main coefficient $\bar{D}_{\text{NiNi}}^{\text{Cu}}$ at the ZFP composition. This observation is consistent with relatively large negative values of $\bar{D}_{\text{NiZn}}^{\text{Cu}}$ compared to the positive $\bar{D}_{\text{NiNi}}^{\text{Cu}}$ values reported for Cu-Ni-Zn alloys.¹⁶

The concept of ZFP for the interdiffusion flux \bar{J}_i based on the Matano coordinate can be extended to fluxes referred to other frames of reference. The flux $(\bar{J}_i)_R$ referred to a frame R moving with a velocity v_R is related to \bar{J}_i by³²

$$(\bar{J}_i)_R = \bar{J}_i - C_i v_R \quad (i = 1, 2, \dots, n) \quad [36]$$

If $v_R = \bar{J}_i/C_i$ for component i at a section within the diffusion zone, $(\bar{J}_i)_R = 0$ at the section and, hence, one can define a ZFP for component i on the frame R . If the frame R is the lattice-fixed frame, *i.e.*, the Kirkendall frame, then a ZFP on this frame is defined for component i at a plane where the Kirkendall velocity coincides with the local mean velocity for the component. Similarly, a ZFP for component i on the solvent-fixed frame implies that the local mean velocity for component i is the same as that of the solvent at the plane of the ZFP. Hence, the ZFP concept is useful in developing insights into diffusional interactions among components on various frames of reference in multi-component diffusion.

IX. COMMENTS AND CONCLUSIONS

The present analysis clearly shows that isothermal multi-component diffusion with solid-solid couples can be investigated for interdiffusion fluxes, zero-flux planes, and flux reversals on the laboratory-fixed frame without the need for a prior knowledge of interdiffusion coefficients. The analysis is facilitated by the use of a relative concentration variable Y_i . The flux Eqs. [7-9] are developed for single phase couples but are applicable to flux calculations in multiphase couples with planar interfaces, provided the molar volumes of all the phases can be considered constant, identical, and independent of composition.

The determination of concentration dependent interdiffusion coefficients \bar{D}_{ij}^n in an n -component system indeed requires the calculation of fluxes as indicated by Eq. [11] and needs $(n - 1)$ diffusion couples with intersecting diffusion paths at a common composition. The flux analysis is complementary to the determination of interdiffusion coefficients. Interdiffusion fluxes, unlike \bar{D}_{ij}^n , are directly determinable quantities from the concentration profiles of an individual couple in an n -component system without the need for invoking Fick's law.

Equations [11] and [12] are applicable to the calculation of interdiffusion coefficients with single phase couples as well as multiphase couples¹⁷ with planar interfaces, provided the molar volume varies little over the diffusion zone.

In the analysis of a single phase solid-solid couple, the presentation of concentration profiles in terms of the relative concentration variable Y_i as a function of x offers several advantages. These are:

1. The concentration profiles of all components are displayed over the diffusion zone L^- to L^+ such that $Y_i = 1$ at L^- and $Y_i = 0$ at L^+ , regardless of the directions of interdiffusion fluxes.
2. The experimental concentration profiles can be checked for internal consistency over the diffusion zone on the basis of Eq. [6] or [17].
3. The location of the Matano plane can be circumvented for the calculation of interdiffusion fluxes on the basis of Eq. [9].
4. The profiles of the individual components intersect at a common cross-over composition Y_c identified at the cross-over plane x_c ; Y_c can be interpreted as the average relative concentration of each component over the diffusion zone, regardless of the directions of their individual interdiffusion fluxes.
5. Y_c and $1 - Y_c$ can be interpreted as the relative depths of diffusion in the two alloys employed in the couple assembly.
6. The location x_c of the cross-over plane relative to the location x_0 of the Matano plane can be described in terms of the concentration profiles of any two of the components.
7. Y_c and the slope of the diffusion path at Y_c are considered to be two characteristic parameters for a ternary, single phase couple and can be employed to represent ternary diffusion paths.²⁶

The calculation of the flux profiles from the concentration profiles as presented in Figure 3 provides a direct appreciation of the magnitudes and directions of the interdiffusion flows of all the diffusing species relative to the Matano coordinate over the entire diffusion zone. The fluxes show a relative maximum or a minimum for each component at the Matano plane. The consistency of the flux calculations can be checked by the requirement that $\sum_{i=1}^n \bar{J}_i = 0$ for the case of constant molar volume.

Another important advantage of the flux profiles lies in the identification of the development of zero-flux planes for the individual components. On the basis of Eqs. [30] and [31], a profile exhibiting a maximum or minimum and indicating equalization of areas as shown in Figure 5 shows the development of a ZFP and flux reversal. The phenomenon of zero-flux planes and flux reversals is quite common in ternary and multicomponent diffusion and has been identified on the laboratory-fixed frame in several Cu-based and Fe-based ternary systems.^{27,33} Not only more than one ZFP can develop for a component but more than one component can show ZFP's within the diffusion zone of a ternary couple depending on the terminal alloys of the couple. For both single phase and multiphase ternary couples, the ZFP compositions have been found to correspond to composition points of intersections of diffusion paths and

isoactivity lines drawn through the terminal alloys on a ternary isotherm.^{27,31,33}

The concept of ZFP and flux reversals can be extended to fluxes based on other frames of reference including lattice-fixed and solvent-fixed frames. The experimental identification of such ZFP's is still to be explored.

ACKNOWLEDGMENT

This research was supported by the United States Department of Energy under contract DE-AC02-81ER10814.

REFERENCES

1. L. Onsager: *Ann. N.Y. Acad. Sci.*, 1945, vol. 46, p. 241.
2. J. S. Kirkaldy: *Advances in Materials Research*, H. Herman, ed., Interscience Publishers, New York, NY, 1970, vol. 4, p. 55.
3. M. A. Dayananda and R. E. Grace: *Trans. TMS-AIME*, 1965, vol. 233, p. 1287.
4. J. S. Kirkaldy, R. J. Brigham, and D. H. Weichert: *Acta Met.*, 1965, vol. 13, p. 907.
5. A. G. Guy and V. Leroy: *The Electron Microprobe*, T. D. McKinley, K. F. J. Heinrich, and D. B. Wittry, eds., John Wiley and sons, 1966, p. 543.
6. T. O. Ziebold and R. E. Ogilvie: *Trans. TMS-AIME*, 1967, vol. 239, p. 942.
7. J. P. Sabatier and A. Vignes: *Mem. Sci. Rev. Metall.*, 1967, vol. 64, p. 225.
8. M. A. Dayananda, P. F. Kirsch, and R. E. Grace: *Trans. TMS-AIME*, 1968, vol. 242, p. 855.
9. A. Vignes and J. P. Sabatier: *Trans. TMS-AIME*, 1969, vol. 245, p. 1795.
10. T. Ericsson: *J. Iron Steel Inst.*, 1970, vol. 208, p. 1109.
11. P. T. Carlson, M. A. Dayananda, and R. E. Grace: *Metall. Trans.*, 1972, vol. 3, p. 819.
12. T. R. Heyward and J. I. Goldstein: *Metall. Trans.*, 1973, vol. 4, p. 2335.
13. A. Brunch and S. Steeb: *Z. Metall.*, 1974, vol. 65, p. 765.
14. R. T. DeHoff, K. J. Anusavice, and C. C. Wan: *Metall. Trans.*, 1974, vol. 5, p. 1113.
15. T. D. Moyer and M. A. Dayananda: *Metall. Trans. A*, 1976, vol. 7A, p. 1035.
16. R. D. Sisson, Jr. and M. A. Dayananda: *Metall. Trans. A*, 1977, vol. 8A, p. 1849.
17. G. H. Cheng and M. A. Dayananda: *Metall. Trans. A*, 1979, vol. 10A, p. 1415.
18. G. W. Roper and D. P. Whittle: *Metall. Sci.*, 1980, vol. 14, p. 21.
19. A. G. Guy and J. Philibert: *Z. Metall.*, 1965, vol. 56, p. 841.
20. H. Fujita and L. J. Gosting: *J. Am. Chem. Soc.*, 1956, vol. 78, p. 1099.
21. C. Bolze, D. E. Coates, and J. S. Kirkaldy: *Trans. ASM*, 1969, vol. 62, p. 794.
22. G. W. Roper and D. P. Whittle: *Metall. Sci.*, 1980, vol. 14, p. 541.
23. M. A. Dayananda, P. F. Kirsch, and R. E. Grace: *Trans. TMS-AIME*, 1968, vol. 242, p. 885.
24. J. I. Goldstein and A. E. Moren: *Metall. Trans. A*, 1978, vol. 9A, p. 1515.
25. C. Wan and R. T. DeHoff: *Acta Met.*, 1977, vol. 25, p. 287.
26. M. A. Dayananda and C. W. Kim: *Scripta Met.*, 1982, vol. 16, p. 815.
27. M. A. Dayananda and C. W. Kim: *Metall. Trans. A*, 1979, vol. 10A, p. 1333.
28. F. J. A. den Broeder: *Scripta Met.*, 1969, vol. 3, p. 321.
29. G. W. Roper and D. P. Whittle: *Scripta Met.*, 1974, vol. 8, p. 1357.
30. G. A. Chadwick and B. B. Argent: *J. Inst. Metals*, 1959, vol. 88, p. 318.
31. C. W. Kim: Ph.D. Thesis, Purdue University, West Lafayette, IN, 1982.
32. D. D. Fitts: *Nonequilibrium Thermodynamics*, McGraw-Hill Book Co., Inc., New York, NY, 1962, p. 5.
33. C. W. Kim and M. A. Dayananda: *Metall. Trans. A*, 1983, vol. 14A, p. 857.